

Deformation Robust Text Spotting with Geometric Prior

Xixuan Hao^{1,2}, Aozhong Zhang¹, Xianze Meng¹ and Bin Fu¹

¹ ShenZhen Key Lab of Computer Vision and Pattern Recognition, Shenzhen Institute of Advanced Technology, Chinese Academy of Sciences

² The University of Hong Kong

hxxjxw@connect.hku.hk, {gz.zhang1, xz.meng, bin.fu}@siat.ac.cn,

Abstract

The goal of text spotting is to perform text detection and recognition in an end-to-end manner. Although the diversity of luminosity and orientation in scene texts has been widely studied, the font diversity and shape variance of the same character are ignored in recent works, since most characters in natural images are rendered in standard fonts. To solve this problem, we present a Chinese Artistic Dataset, termed as ARText, which contains 33,000 artistic images with rich shape deformation and font diversity. Based on this database, we develop a deformation robust text spotting method (DR TextSpotter) to solve the recognition problem of complex deformation of characters in different fonts. Specifically, we propose a geometric prior module to highlight the important features based on the unsupervised landmark detection sub-network. A graph convolution network is further constructed to fuse the character features and landmark features, and then performs semantic reasoning to enhance the discrimination for different characters. The experiments are conducted on ARText and IC19-ReCTS datasets. Our results demonstrate the effectiveness of our proposed method.

1 Introduction

Spotting text, aiming at detecting and recognizing text in an end-to-end manner, is an emerging topic in the computer vision community, due to the wide application in machine translation, image retrieval and autonomous driving. In recent years, it has achieved significant progress due to the rapid development of deep neural networks. The diversity of texts is the critical challenge for text spotting tasks, and various methods [Xing *et al.*, 2019; Wang *et al.*, 2020a; Liao *et al.*, 2020; Liu *et al.*, 2021a; Wang *et al.*, 2021; Huang *et al.*, 2022] have been proposed to handle the diversity problem of luminosity and orientation in scene texts. Unfortunately, we find the intrinsic diversity of characters, namely the font diversity, has been almost ignored in recent studies, where the large variance of shape of the same character in various fonts may cause significant performance degradation in reading texts.

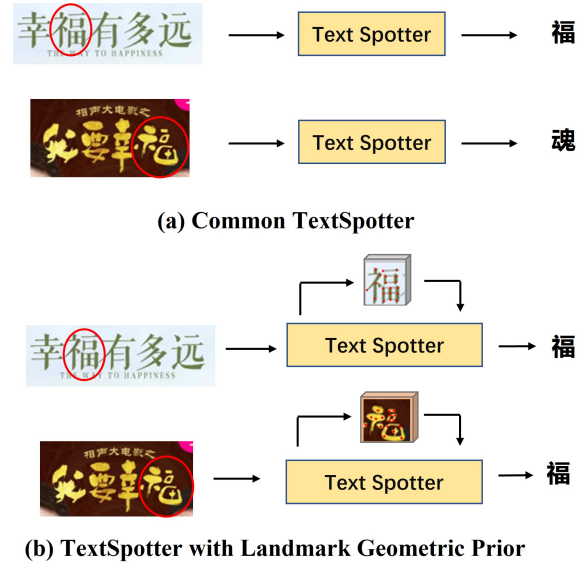


Figure 1: The illustration of our motivation. (a) is the recognition result of common text spotter, (b) is the recognition result of our proposed method. For characters with rich shape deformation, (a) is tend to misrecognize the content. For example, “福” in standard font can be recognized correctly in the top line of (a), but “福” in the complex font is misrecognized as “魂” in the bottom line of (a). With geometric prior, our model can get more information about the basic architecture of characters, thus being more capable of recognizing characters with diversified fonts. For example, “福” in the complex font is recognized correctly in the bottom line of (b).

Since the font of characters in most scene text images is still close to the standard fonts, the importance of font diversity receives limited attention. To illustrate the above problem, we perform experiments on the generalization ability for text spotting in complex font scenarios. We select 100 kinds of Chinese fonts, including simple, medium and hard categories, then split them randomly into two sets A and B, each set contains 50 fonts (the proportion of simple, medium and hard fonts remains the same 8 : 11 : 6 in two sets). We utilize A set font to generate 50,000 text images, then split them as 40,000 images in training set and 10,000 images in testing set. Based on the testing images in A set, we randomly select fonts in B set and generate test images with the same content of testing images in A set. Then we optimize AE

	Detection	1-NED	1-NED			N_1	N_2	Font Difficulty Distribution		
A set	0.993	0.977	simple	medium	hard	8960	1923	simple	medium	hard
			0.984	0.978	0.965					
B set	0.990	0.918	simple	medium	hard	7623		289	299	935
			0.971	0.953	0.781					

Table 1: Experiments on generalization ability for text spotting in complex font scenarios. We use the edit-distance-based metric, 1-NED, to evaluate the recognition performance. N_1 stands for the Number of completely recognized images. N_2 stands for the Number of A-right-B-wrong image pairs. Font Difficulty Distribution represents font difficulty distribution of A-right-B-wrong images.

TextSpotter [Wang *et al.*, 2020a] on training images and test the recognition performance on testing images of A set and B set respectively. As shown in Table 1, the recognition performance has dropped by about 6% on B testing set whose fonts are never seen before by the model, while the detection performance remains almost the same, which illustrates that the performance degradation is caused by the recognition part. We also summarize the number of A-right-B-wrong image pairs in Table 1 and analyze the image font difficulty distribution of misrecognized images, finding that the probability of inaccurate recognition increases with font difficulty. Therefore, the font diversity is a significant challenge for current textspotter models. Besides, the difficulties and challenges of font diversity are discussed in [Xie *et al.*, 2022], which can also support our conclusion.

In this paper, to solve the above problems, we propose a **Chinese Artistic Text Dataset**, termed as ARText, which focuses on the font diversity and shape variance of characters in text spotting. The ARText dataset contains 33,000 images collected on the Internet with rich shape deformation and font diversity, and has been randomly divided into training set (30,000 images) and testing set (3,000 images) for model development. The character-level and text-level annotations are both provided, including the bounding boxes and the corresponding content, which can be utilized in text detection, text recognition and text spotting tasks. The detailed annotation strategy and statistic information will be discussed in Section 3.

Based on this dataset, we develop a deformation robust text spotting method (DR TextSpotter) to solve the recognition problem caused by complex shape deformation and font variance, as shown in Figure 1. Specifically, motivated by the fact that the basic geometric relations of the same character are preserved in different fonts, we introduce the geometric prior to highlight the important features through the unsupervised landmark detection sub-network. Moreover, due to the sparse nature of landmark-based features, we embed all features into graph space, then the graph convolution network is utilized to perform semantic reasoning. With the geometric prior, the graph convolution can effectively encode landmark information, which will enhance the discrimination of inter-character features and the stability of intra-character features, thus improving the recognition ability for characters with diversified fonts. To demonstrate the effectiveness of our proposed method, we conduct experiments on ARText dataset and widely-used IC19-ReCTS dataset. Experimental results show our method achieves state-of-the-art performance on

IC19-ReCTS dataset [Zhang *et al.*, 2019], and outperforms its counterparts about 1.5% in terms of the edit-distance-based evaluation metric (1-NED) on our ARText dataset.

The main contributions are summarized as follows: 1) We construct a Chinese artistic text dataset, namely ARText, which is a Chinese dataset focusing on the font diversity and shape variance of characters in the text spotting task. 2) We propose a novel network architecture Deformation Robust TextSpotter, which employ geometric prior and graph neural network to enhance the discrimination of inter-character features and the stability of intra-character features. 3) Experimental results demonstrate the effectiveness of DR TextSpotter. On ARText dataset, DR TextSpotter achieves state-of-the-art performance, surpassing other methods by about 1.5% in terms of 1-NED.

2 Related Work

2.1 Scene Text Spotting

Scene Text Spotting [Li *et al.*, 2017; Liu *et al.*, 2018; Lyu *et al.*, 2018; Qin *et al.*, 2019; Xing *et al.*, 2019; Liu *et al.*, 2020; Wang *et al.*, 2020a; Feng *et al.*, 2019; He *et al.*, 2018; Baek *et al.*, 2020; Wang *et al.*, 2021; Huang *et al.*, 2022] is commonly composed of two subtasks: text detection [Xu *et al.*, 2022b; Su *et al.*, 2022; Xu *et al.*, 2022a] and text recognition [Li *et al.*, 2022b; Li *et al.*, 2021; Peng *et al.*, 2022]. In the past years, the rise of deep learning and the great advances in object detection have promoted the prosperity of this field. [Li *et al.*, 2017] first used RoI Pooling to correlate detection and recognition features via end-to-end training, but it can only handle horizontal and centralized text. Inspired by the Mask R-CNN, Mask TextSpotter [Liao *et al.*, 2020] addressed text of various shapes with the help of instance segmentation. ABCNet [Liu *et al.*, 2021a] introduced Bezier curves and new sampling methods (BezierAlign) to localize oriented and curved scene text. AE TextSpotter [Wang *et al.*, 2020a] added linguistic representation to text detection to solve the ambiguity problem and designed a novel text recognition module to achieve fast recognition. PAN++ [Wang *et al.*, 2021] utilized kernel representation to achieve arbitrarily-shaped text spotting. Recently, as the Transformer architecture [Vaswani *et al.*, 2017] begins to sweep into the Computer Vision community from Natural Language Processing area, there are also some transformer-based text spotting works emerging. For example, Swin TextSpotter [Huang *et al.*, 2022] first introduced Swin Transformer [Liu *et al.*, 2021b] backbone into end-to-end text spotting and achieves promising results. [Xie

Types \ Difficulty	TV Series	Movie	Variety Show	Comic	Children	Documentary	UGC	Total
Simple	68	6	16	19	0	0	7955	8064
Medium	4527	2158	871	657	775	907	5212	15107
Hard	3499	2450	1097	1431	727	539	86	9829
Total	8094	4614	1984	2107	1502	1446	13253	33000

Table 2: Statistics for the ARText dataset.

et al., 2022] used cross-attention to merge the encoded image feature and corner map feature.

In these methods, however, the importance of geometric prior in text spotting was ignored. In this work, we introduce landmarks as geometric information to achieve deformation robust text spotting.

2.2 Geometric Prior

A vast amount of literature indicates that geometric priors can help deep learning models improve performance, such as shape completion[Dai *et al.*, 2017], position embedding[Vaswani *et al.*, 2017] and landmark detection. Landmark detection is often used as a kind of structural information to assist network learning. For instance, there are many traditional methods on human faces such as active appearance models [Cristinacce and Cootes, 2008], template-based methods [Pedersoli *et al.*, 2014] and regression-based methods [Cao *et al.*, 2014]. After the rise of deep learning, more accurate landmark localization and better performance can be achieved [Wu *et al.*, 2017; Xia *et al.*, 2022; Li *et al.*, 2022a]. In addition to human faces, landmark detection is also widely applied to Camera Localization [Do *et al.*, 2022], medical image analysis [Yin *et al.*, 2022], 3D Face Reconstruction [Wood *et al.*, 2022]. In this work, We regard landmarks as geometric information of characters to improve model generalization.

2.3 Graph Reasoning

Graph-based approaches are efficient relational reasoning methods, which have become popular in various deep learning tasks in recent years. [Kipf and Welling, 2016] first proposed graph convolution neural networks and applied them to semi-supervised learning. Owing to the ability to capture global information through graph propagation, graph reasoning is introduced for visual understanding tasks [Yao *et al.*, 2021; Zhao *et al.*, 2021; Wang *et al.*, 2020b; Chen *et al.*, 2019]. Moreover, [Li and Gupta, 2018] and [Chen *et al.*, 2019] adopted graph convolution reasoning to build an end-to-end module for reasoning between disjoint and distant regions. Inspired by these works, we employ the reasoning power of graph convolutions to fuse character features with corresponding landmark features.

3 Chinese Artistic Dataset

Our proposed ARText dataset consists of 33,000 Chinese artistic images collected from the Internet. The data source, annotation details, data statistics are described below.

Data Source: We collect our ARText images all from the Internet, trying to cover a wide content range. Then we impose data cleaning manually on them, removing images with low-resolution or inappropriate content. Finally, we categorize these images into different types as UGC (User Generated Content), Movies, TV Series, Children, Comic, Variety Show and Documentary.

Annotation Details: In each annotation, we provide text-level bounding box and character-level bounding box with their contents. The format of the bounding box includes four corner points of the orientated bounding box. In one image, there may be multiple texts in different font sizes, but we only focus on the main part and ignore some small texts.

Dataset Analysis: The whole dataset includes 33,000 images with 3563 different kinds of Chinese characters. The dataset statistics can be seen on Table 2. We label dataset images into three categories (Simple, Medium, Hard) manually, according to the recognition difficulty standard, as described in Table 3. The examples are shown in Figure 2. Moreover, we calculate the occurrence frequency of each character in both training set and testing set. The top-30 characters are presented in Figure 3, and the character frequency distribution of training and testing set basically remains the same. We also calculate the text length distribution of the whole dataset, which is shown in Figure 4. Note that there might be multiple text instances in one image, so the image counts can be larger than ARText image number.

Font	Standard
Simple	The font has no decoration, and its glyph has almost no deformation compared to standard fonts.
Medium	The font has no decoration, and its glyph has deformation compared to standard fonts.
Hard	The font has rich decoration, and its glyph has deformation compared to standard fonts.

Table 3: Font classification standard.

4 Methodology

4.1 Overall Pipeline

The overall pipeline of our Deformation Robust TextSpotter is shown in Figure 5, which mainly consists of Feature Extraction stage, Proposal Generation and Extraction stage, Text Detection Branch, and Character Recognition Branch. We implement the Region Proposal Network (RPN) [Ren *et al.*, 2015] on top of ResNet-50 [He *et al.*, 2016] as the Feature



Figure 2: Examples of image difficulty categories. (a)(b) are simple, (c)(d) are medium, (e)(f) are hard.

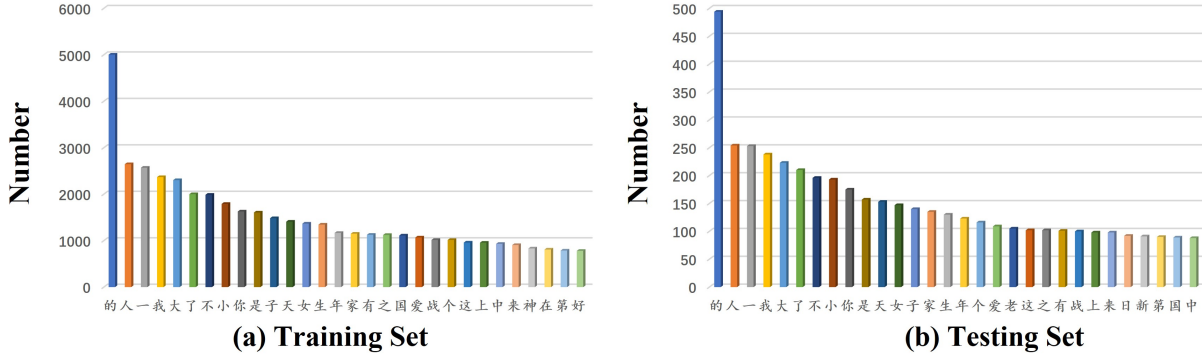


Figure 3: Statistics of top-30 frequent characters in the training set (a) and testing set (b).

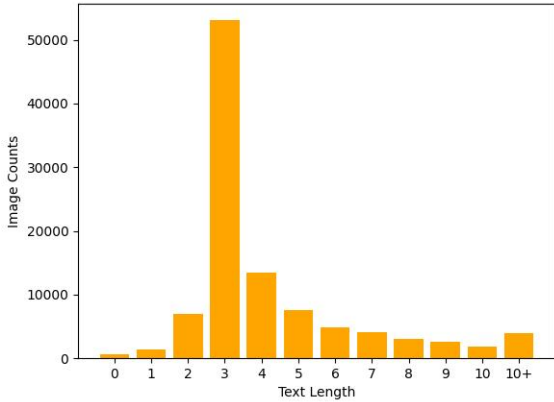


Figure 4: Text length distribution of ARTText.

Extraction stage to predict text line proposals and character proposals. The ROIAlign is utilized as Proposal Generation and Extraction stage to crop the resulting proposal regions and reshape them into the predefined size. For the text proposal, Text Detection Branch predicts the probability of this region and further refines the text location with the oriented bounding boxes. For the character proposal, RoIAlign[He *et al.*, 2017] transformed the character proposal to character feature maps F_c and \mathcal{H} with different sizes, then pass

them into the Character Recognition Branch. The Geometric Prior Module (GPM) is proposed to generate a predefined number of landmark features \mathcal{H}_k according to the predicted positions. The landmark features and the character features F_c are passed to the Graph Reasoning Module (GRM), which performs graph convolution to reason semantic relations under geometric prior. The resulting features will be further fed to Detection Head to predict characters and bounding boxes. Finally, we assemble characters according to the Intersection-over-Union (IOU) between the predicted text line (generated by the detection branch) and the character bounding box.

4.2 Geometric Prior Module

As we discussed in the previous section, although the large shape variance and font diversity exist in the same kind of characters, the basic token relations will remain unchanged. Based on this motivation, we propose the Geometric Prior Module (GPM) to highlight the critical shape information in character features.

In this work, the central insight of GPM is that the geometric relations in each character can be summarized by a set of key points. Based on this insight, we build a landmark detection sub-network on top of the character feature patches $\mathcal{H} \in R^{70 \times 70 \times D}$ (D denotes feature dimension), which consists of three 3×3 convolutional layers (the first one layer is with stride 2 and the last two layer is with stride 1). The first two convolutional layers are followed by Batch Normalization and ReLU, while the last convolutional operator fol-

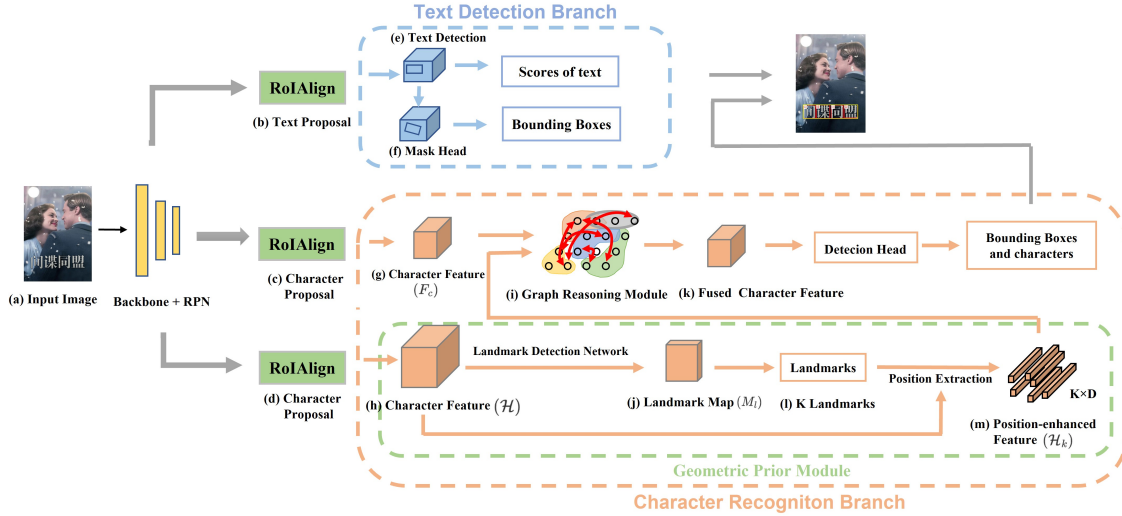


Figure 5: Overall Architecture of DR TextSpotter, which mainly consists of Feature Extraction stage (Backbone + RPN), Proposal Generation and Extraction stage (ROIAlign), Text Detection Branch, and Character Recognition Branch.

lowed by the softmax function predicts the landmark map $M_l \in R^{35 \times 35 \times K}$ (K is the number of landmarks), where the position of the maximum value in each channel m indicates the position of the m -th landmark. Then we use softmax operation to get the corresponding landmarks, and extract features at landmark position from the original character feature $\mathcal{H} \in R^{70 \times 70 \times D}$, obtaining the landmark features $\mathcal{H}_k \in R^{K \times D}$.

Due to the lack of landmark annotation in the existing text spotting dataset, the training process of GPM is a challenging task. As shown in Figure 6, We develop an unsupervised training strategy to remedy this problem. Since the landmarks are the most remarkable positions for each character, we may expect that the GPM will find the same landmarks after random perturbations. In other words, the landmark has the characteristic of transformation equivariance. Therefore, once we obtain the character feature patch $\mathcal{H} \in R^{70 \times 70 \times D}$, we generate another feature patch $\hat{\mathcal{H}} \in R^{70 \times 70 \times D}$ by three kinds of geometric transformation g : rotation, translation and scaling. The feature maps \mathcal{H} and $\hat{\mathcal{H}}$ are both passed to the Landmark Detection Network to generate landmark maps M_l and \hat{M}_l , respectively.

We apply unsupervised optimization objections to train GPM. The first optimization target is the alignment loss:

$$L_{landmark}^{align} = \frac{1}{K} \sum_{r=1}^K \sum_{u,v} ||u - g(v)||^2 M_l(u|\mathcal{H}, r) \hat{M}_l(v|\hat{\mathcal{H}}, r) \quad (1)$$

where u and $v \in \{1 \dots H\} \times \{1 \dots W\}$ indicates location, g denotes feature geometric transformation. K denotes the number of landmarks. $M_l(u|\mathcal{H}, r)$ is the landmark maps. r denotes the channel of landmark map M_l .

In practice, implementing Equation 1 is computation inefficient, so we decompose the loss as a format of linear time complexity [Thewlis *et al.*, 2017]:

$$\sum_u ||u||^2 M_l(u|\mathcal{H}, r) + \sum_v ||g(v)||^2 M_l(v|\hat{\mathcal{H}}, r) - 2 \left(\sum_u u M_l(u|\mathcal{H}, r) \right)^T \cdot \left(\sum_v g(v) M_l(v|\hat{\mathcal{H}}, r) \right) \quad (2)$$

With the Equation 2, the landmark detection network may come to a trivial solution, where all landmarks converge into a single position. To solve this issue, we apply the second optimization objection, the diversity loss [Thewlis *et al.*, 2017]:

$$L_{landmark}^{div} = K - \sum_{r=1, \dots, K} \max_u M_l(u|\mathcal{H}, r) \quad (3)$$

This loss imposes penalties to the overlap of the max value of landmark probability map, thus preventing the network from learning K identical landmarks. In practice, we utilize a downsampling operation (4×4 average pooling) before applying the diversity loss to encourage further landmark extraction.

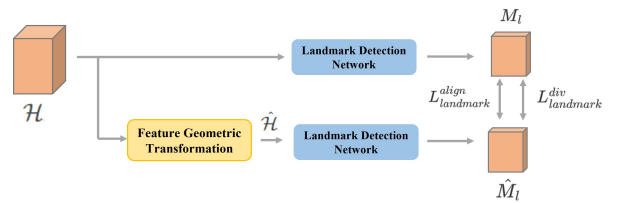


Figure 6: Geometric Prior Module in Unsupervised Training Process.

4.3 Graph Reasoning Module

Since the landmark feature $\mathcal{H}_k \in R^{K \times D}$ is the non-grid feature, we construct the graph structure to perform global semantic reasoning in the interaction space. Inspired by GloRe

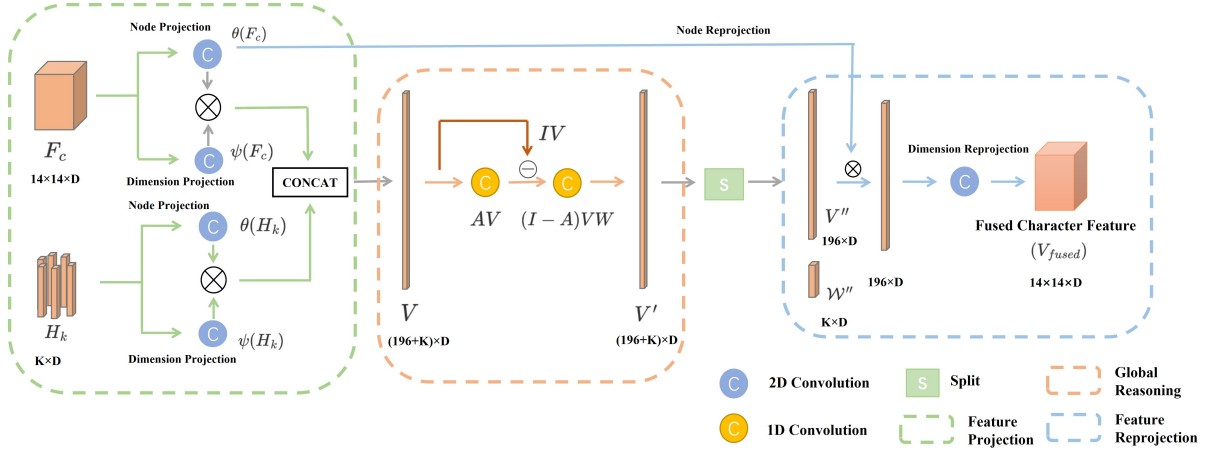


Figure 7: The architecture of GRM. GRM includes three steps: Feature Projection, Global Reasoning and Feature Rejection. For simplicity, the convolution layers are utilized to implement Projection, Global Reasoning and Rejection operations.

unit [Chen *et al.*, 2019], the process of our GRM can be summarized in three steps, as shown in Figure 7.

1) Feature Projection: Firstly, we need to transform character features F_c and landmark features \mathcal{H}_k to interaction space.

For input features $X \in \mathbb{R}^{L \times C}$, our goal is to find a map function to project X to the new features $Z = f(X) \in \mathbb{R}^{N \times C'}$ in the interaction space, where C and C' are the feature dimension, and we set $C = C'$ in this module. $L = W \times H$ is the position dimension and N is the number of features in interaction space.

$$z_i^q = w_i^q X = \sum_{\forall j} w_{ij}^q x_j \quad (4)$$

with learnable weights $W_p^q = [w_1^q, \dots, w_N^q]$, $w_i^q \in \mathbb{R}^L$; $X = [x_1, \dots, x_N]$, $x_j \in \mathbb{R}^C$, where $q \in \{c, k\}$ denotes the weight for F_c or \mathcal{H}_k . In practice, we implement $f(X)$ into two functions, $\psi(X; W_\psi^q)$ for dimension projection and $W_p^q = \theta(X; W_\theta)$ for node projection.

$$f(X) = \theta(X; W_\theta^q) \times \psi(X; W_\psi^q) \quad (5)$$

The function $\psi(\cdot)$ and $\theta(\cdot)$ are implemented by a 1×1 2D convolution layer respectively. “ \times ” denotes the matrix multiplication operation.

After projecting $F_c \in \mathbb{R}^{14 \times 14 \times D}$ and $H_k \in \mathbb{R}^{K \times D}$ to the interaction space, we concatenate them together and get $V \in \mathbb{R}^{(196+K) \times D}$.

2) Global Reasoning: We perform semantic reasoning to embed geometric prior into features through graph convolution [Chen *et al.*, 2019]

$$U = GZW_r = (I - A)ZW_r \quad (6)$$

where G and A stand for adjacent matrix, W_r is the weight matrix for state updating, which can be achieved by two 1D convolutions aligning both channel and node direction [Chen *et al.*, 2019] as shown in Figure 7.

After global reasoning, we get $V' \in \mathbb{R}^{(196+K) \times D}$, then we split the feature V' into the character feature V'' and landmark feature W'' . Finally, we reproject character feature $V'' \in \mathbb{R}^{196 \times D}$ back to coordinate space.

3) Feature Rejection: To make the output features of GRM can be well utilized in the subsequent recognition, the last step is to project the output features back to the original space. Rejection can be formulated as

$$y_i = \phi_i V'' = \sum_{\forall j} \phi_{ij} v_j'' \quad (7)$$

where $\Phi = [\phi_1, \dots, \phi_L]$, $\phi_i \in \mathbb{R}^N$. In practice, we implement the above rejection function into two functions, σ for dimension rejection and δ for node rejection:

$$h(V'') = \sigma(\delta \times V''; W_\sigma) \quad (8)$$

The function $\sigma(\cdot; W_\sigma)$ is implemented by a 1×1 2D convolution layer and W_σ denotes the learnable weight. We set $\delta = (W_p^c)^T$ (i.e. reuse the projection weight generated in the first step) to save computation.

4.4 Optimization

The training process of DR TextSpotter is divided into three stages: In the first stage, we optimize the backbone network, Region Proposal Network (RPN), Text Detection Branch (TDB) and Character Recognition Branch (CRB) by a joint loss of L_{TDB} and L_{CRB} . In the second stage, we train the Geometric Prior Module (GPM) by $L_{landmark}^{align}$ and $L_{landmark}^{div}$. In the third stage, we fix the weight of GPM and remove the weight of the classification layer in the Detection Head of Character Recognition Branch (CRB), then finetune the whole network.

Correspondingly, the loss function can be divided into two parts: 1) The detection and recognition loss function. 2) The landmark detection loss function.

The detection and recognition loss function: $L_{Spotting}$ is a multi-task loss function which is used to optimize the backbone network, RPN, TDB and CRB (without GPM).

$$L_{Spotting} = L_{RPN} + L_{TDB} + L_{CRB} \quad (9)$$

where L_{RPN} is loss function of RPN as defined in [Ren *et al.*, 2015]. L_{TDB} and L_{CRB} are loss functions for TDB and CRB (without GPM) respectively, which can be formulated as

$$L_{TDB} = L_{TDB}^{cls} + L_{TDB}^{bbox} + L_{TDB}^{mask} \quad (10)$$

$$L_{CRB} = L_{CRB}^{cls} + L_{CRB}^{bbox} \quad (11)$$

where L_{TDB}^{cls} and L_{CRB}^{cls} are cross-entropy loss for text/non-text classification and character classification, respectively. L_{TDB}^{bbox} and L_{CRB}^{bbox} are smooth L1 loss for bounding box regression in TDB and CRB respectively. L_{TDB}^{mask} is the binary cross-entropy loss of mask head in TDB.

The landmark detection loss function: $L_{landmark}$ is used to implement equivariance constraint for landmark detection network

$$L_{landmark} = L_{landmark}^{align} + \lambda L_{landmark}^{div} \quad (12)$$

where $L_{landmark}^{align}$ is the probability map loss to learn equivariance constraint, while $L_{landmark}^{div}$ is the diversity loss to prevent the network from learning K identical copies of the same landmark, as defined in Section 4.2. We empirically set $\lambda = 50$ to balance the above two loss functions.

5 Experiments

In this section, we first introduce the datasets and metrics, then compare our model with existing state-of-the-art methods. Finally, we conduct ablation studies to verify the effectiveness of different modules.

5.1 Datasets

Chinese Artistic Text dataset: To solve the problems about the font diversity and shape variance in text spotter, we propose the Chinese Artistic Text dataset, which provides 30,000 text images for training and 3,000 images for testing. The detailed description is provided in Section 3.

IC19-ReCTS dataset: IC19-ReCTS dataset [Zhang *et al.*, 2019] is proposed in ICDAR 2019 Robust Reading Challenge on Reading Chinese Text on Signboard. There are 25,000 labeled images, including 20,000 images for training and 5,000 images for testing.

5.2 Implementation Details

The parameter settings in the backbone, RPN, and Text Detection Branch are the same as AE TextSpotter [Wang *et al.*, 2020a]. The magnitudes of geometric transformations in GPM are randomly selected by: Rotation $\in (0, 2\pi)$, Translation $\in (-0.2, 0.2)$, and Scaling $\in (0.7, 1.3)$. In GRM, the number of landmarks K is set to 16, D is set to 256, the number of nodes and dimensions in interaction space is set the same as the original coordinate space. In the training process, we first optimize the backbone network, RPN, TDB, and CRB with batch size 8 on 4 Quadro RTX-8000 GPUs for 12 epochs. Secondly, we optimize the Geometric Prior Network (GPM) and freeze other layers. Finally, we remove the weight of classification layers in the Detection Head of CRB,

then finetune the whole network. We optimize all models using stochastic gradient descent (SGD) with a weight decay of 1×10^{-4} with the momentum 0.9. The initial learning rate is 0.02, which will be divided by 10 at epoch 8 and 10. The random scale, random horizontal flip, and random crop are utilized as data augmentation strategies in the training stage.

5.3 Metrics

The Precision, Recall and F-measurement are computed based on detection results. Moreover, we use normalized edit distance (NED) based metric to evaluate end-to-end recognition performance, which is defined as:

$$1-NED = 1 - \frac{1}{N} \sum_{i=1}^N \frac{L(T_i, \hat{T}_i)}{\max(|T_i|, |\hat{T}_i|)} \quad (13)$$

where L denoted the Levenshtein Distance, T_i represents the predicted text and \hat{T}_i represents the corresponding ground truth, $|T_i|$ and $|\hat{T}_i|$ represent the length of corresponding texts, N is the total number of text lines.

5.4 Comparisons with State-of-the-Art Methods

To further demonstrate the effectiveness of the proposed DR TextSpotter, we compare it with existing state-of-the-art methods on our ARText dataset and widely-used IC19-ReCTS dataset [Zhang *et al.*, 2019], respectively. We choose AE TextSpotter [Wang *et al.*, 2020a], Mask TextSpotter v3 [Liao *et al.*, 2020], ABCNet v2 [Liu *et al.*, 2021a] and SwinTextSpotter [Huang *et al.*, 2022] as the representative methods. For the ARText dataset, we utilize the officially released codebase to train and evaluate each model. As shown in Table 4, our DR Textspotter outperforms baseline (AE TextSpotter without LM) with about 2.5% and outperforms existing state-of-the-art method (SwinTextSpotter) about 1.5% in terms of normalized edit distance. It is also worth mentioning that, with the language model, the performance of AE TextSpotter is slightly dropped, since the length of texts in ARText dataset is much shorter than the traditional scene text dataset. As shown in Table 5, we validate our DR TextSpotter on public-available IC19-ReCTS [Zhang *et al.*, 2019] dataset, where our proposed model achieves the best record 73.20% in terms of 1-NED. We also conduct experiments on English dataset, the results are shown in Section 5.11.

5.5 Ablation Study for Geometric Prior Module

The unsupervised optimization objection

In Geometric Prior Module (GPM), we utilize $L_{landmark}^{align}$ and $L_{landmark}^{div}$ to constrain the training of the Landmark Detection Network. As mentioned in Section 4.2, $L_{landmark}^{align}$ is the probability alignment loss to learn equivariance constraint while $L_{landmark}^{div}$ is the diversity loss to prevent the network from learning K identical landmarks. To investigate the function of the above loss functions, we perform ablation studies on our ARText dataset, and the experimental results are presented in Table 6. Although the main task of training Landmark Detection Network is implemented by $L_{landmark}^{align}$, the presence of $L_{landmark}^{div}$ has a greater impact on model performance. Because if only $L_{landmark}^{align}$ exists, the network

Methods	Detection			E2E	FPS	Params
	P	R	F	1-NED		
Mask TS v3	85.65	62.55	72.30	54.82	2.5	57.43M
ABCNet v2	88.62	87.37	87.99	66.72	10.0	48.16M
AE TS w/o LM	88.15	89.13	88.64	72.12	1.8	256.0M
AE TS	87.97	88.97	88.47	72.06	2.5	224.7M
SwinTS*	92.44	89.82	90.15	73.22	0.2	225.4M
DR TS (Ours)	92.48	88.67	90.53	74.69	1.5	236.4M

Table 4: Results on ARText dataset. "TS" denotes TextSpotter, while "LM" denotes the language module, and E2E means end-to-end text spotting result. * denotes that, to ensure a fair comparison, we make the parameters of Swin TextSpotter roughly equivalent to our model, by modifying pooler resolution and adding some convolution layers.

Methods	Detection			E2E	FPS	Params
	P	R	F	1-NED		
Mask TS v2	89.30	88.77	89.04	67.79	2.0	80.13M
ABCNet v2	93.60	87.50	90.40	62.71	10.0	48.16M
AE TS w/o LM	91.54	90.78	91.16	71.10	2.5	224.7M
AE TS	92.60	91.01	91.80	71.83	1.8	256.0M
SwinTS*	94.15	87.19	90.57	72.58	0.2	225.4M
DR TS (Ours)	94.47	90.06	92.21	73.20	1.5	236.4M

Table 5: Results on IC19-ReCTS dataset. "TS" denotes TextSpotter, while "LM" denotes language module, and E2E means end-to-end text spotting result. * denotes that, to ensure a fair comparison, we make the parameters of Swin TextSpotter roughly equivalent to our model, by modifying pooler resolution and adding some convolution layers.

tends to meet $L_{landmark}^{align}$ constraint by learning K identical landmarks, where the landmarks can not provide effective information for recognition. We also conduct experiments on GPM, as is shown in Table 6, when remove GPM, only keep the character feature F_c ((g) in Figure 6) for Graph Reasoning Module, the performance drops about 2.3%, which shows the effectiveness of landmarks.

5.6 Ablation Study for Graph Reasoning Module

The function of the graph reasoning module is to effectively fuse the character feature and landmark feature. In order to study the effectiveness of this model, we select two other common approaches for comparison: Concatenation and Summation. 1) For the concatenation case, we directly concatenate the landmark feature (Figure 5 (m)) and the character feature (Figure 5 (g)), then pass the fused feature to the Detection Head. 2) For the summation case, we bilinear interpolation Landmark Map (Figure 5 (j)) to the size of Character Feature (Figure 5 (g)), and get the mean value of K channels, then sum them to the Character Feature (Figure 5 (g)) for subsequent recognition.

To avoid the performance gains due to the large number of

Methods	Detection			E2E
	P	R	F	1-NED
DR TS w/ L1 w/o L2	91.13	88.40	89.51	73.20
DR TS w/o L1 w/ L2	90.72	88.82	89.83	73.55
DR TS w/o GPM	88.93	67.37	75.48	72.38
DR TS (ours)	92.48	88.67	90.53	74.69

Table 6: Ablation study for unsupervised optimization objection on ARText. The L_1 and L_2 represent $L_{landmark}^{align}$ and $L_{landmark}^{div}$, respectively. "TS" denotes TextSpotter.

parameters, we make sure that the ablation experiments parameters are not less than DR TextSpotter by adding several layers of convolutions. The experimental results are shown in Table 7, and we can draw the following conclusions: 1). Concatenation is proven to be useful, but not as effective as the graph method in terms of F-measurement and 1-NED. 2). Although Concatenation performs better on Precision, its parameters far exceed other models, as well as computation volume and memory consumption. 3). Summation method, however, make performance degrade in terms of 1-NED, even lower than baseline (AE TextSpotter w/o LM). We think the reason may come from that character feature and landmark feature distribute in different feature space, direct summation only leads to an increase in value but does not make any sense in theory. 4). The GRM achieves the best recognition performance in terms of 1-NED, which verifies the effectiveness of the graph reasoning module.

Methods	Detection			E2E	Params
	P	R	F	1-NED	
Concatenation	92.84	87.62	90.15	74.16	252.21M
Summation	91.15	88.41	90.34	71.88	236.53M
GRM (ours)	92.48	88.67	90.53	74.69	236.37M

Table 7: Abalation study for feature fusion method on ARText.

5.7 Ablation study on Landmark Numbers

To choose the best number of landmarks, we do experiments with 4, 8, 16, 24 landmarks on our ARText dataset and keep other settings unchanged. As shown in Table 8, the performance improves as the landmark number increases until $K = 16$ in terms of 1-NED. We think the reason comes from the unsupervised optimization strategy, where the generated landmarks may contain noise. As the number of landmarks increases, the noise will accumulate. Moreover, if fewer landmarks are utilized, it is not enough to cover all important positions in character. Therefore, only the appropriate number of landmarks can make the model work best.

5.8 Visualization Results of Landmark Locations

The visualization results of the landmark are shown in Figure 8. The landmarks are mainly distributed in the important positions of the character, such as the start, end and bend positions, thus can provide useful geometric information for the

Landmark Numbers	Detection			E2E
	P	R	F	1-NED
4 landmarks	91.04	88.52	90.04	73.52
8 landmarks	92.45	87.97	90.21	74.06
16 landmarks (ours)	92.48	88.67	90.53	74.69
24 landmarks	93.28	85.95	90.07	73.83

Table 8: Ablation study for landmark number on ARText.

recognition model. However, the landmark positions are not particularly accurate, because of the unsupervised learning method. Actually, how to produce stable and effective landmarks is an open question and our work provides one possible direction.



Figure 8: Visualization results of Landmarks. Landmarks can outline the structure of the character, thus providing information to correct wrong recognition due to complex font.

5.9 Visualization Results on ARText Dataset

Figure 10 presents the visualization results of the text spotting model. Compared with the baseline model (AE TextSpotter [Wang *et al.*, 2020a] without language model), our proposed model can correctly recognize hard characters with complex fonts, which illustrates the robustness of our model to solve the large shape variance problem.

5.10 Failure Cases and Limitations

Although our model achieves state-of-the-art performance, it still fails in some special cases. Some posters are carefully designed in order to highlight the visual effect, thus can result in two main problems: Character overlap and Complex layout, corresponding to Figure 9 (a) and (b)(c). 1. When different text lines are arranged closely or even cross with each other, it will cause difficulties for the model in both detection and recognition. 2. The complex layout is another serious issue in artistic text spotting. The model cannot arrange each character into the appropriate order, resulting in misrecognition.

Besides, to train our model, we need character-level annotations, which are not easy to transfer to other datasets. This can be solved by semi-supervised training scheme [Xing *et al.*, 2019]: (1) Use the SynthText tool to generate a synthetic dataset with character-level annotations. (2) Pre-train model on the synthetic dataset. (3) Finetune the model on the

Methods	Detection			E2E
	P	R	F	1-NED
Mask TextSpotter v3	84.12	73.23	78.30	56.61
AE TextSpotter w/o LM	84.15	73.66	78.55	53.84
SwinTextSpotter	86.29	80.70	83.40	57.04
DR TextSpotter (Ours)	88.96	79.36	83.89	57.96

Table 9: Results on ReCTS-Eng dataset. “P”, “R”, “F” and “1-NED” mean the precision, recall, F-measure, and the edit-distance-based evaluation metric, respectively. “LM” denotes the language module. E2E means end-to-end text spotting result

target dataset with text-level annotations by gradually identifying the “correct” char-level bounding boxes from real-world images by the model itself. Specifically, when fine-tuning on the real dataset, the model collects the “correct” char-level bounding boxes detected in real-world images, which are used to further train the model. However, in our model, each character needs to be fed into Character Recognition Branch, including GPM, GRM and Detection Head, which is time-consuming for performing pre-training or semi-supervised schemes to train a text spotting model for the languages (such as English) with many characters in each text instance. In summary, for the languages (such as Chinese and Japanese) with few characters in each text instance, even without character-level annotations, we can generate a synthetic dataset with character-level annotations, and then perform semi-supervised scheme to train our text spotting model. For the languages (such as English) with many characters in each text instance, training our model under semi-supervised scheme will take a long time, thus the character-level annotations are needed to optimize our model.

In this paper, we only focus on the font diversity problem in this work, since many plug-and-play modules have been proposed to solve the orientation problem [Shi *et al.*, 2018; Wang *et al.*, 2019; Baek *et al.*, 2019], which can be incorporated into our models.

5.11 Results on English dataset

Based on the discussion in Section 5.10, we cannot conduct experiments on common English datasets. However, to further verify the effectiveness and generalization of our proposed method, we select images with English annotations from IC19-ReCTS dataset and set “ignore” label True for Chinese content in the images. Then we get 10,308 images with 22,135 English text annotations and 147,062 English character annotations. We split into training set and testing set by 8:2. We train our model and other state-of-the-art methods (without pre-training) on the ReCTS-eng dataset, the results can be seen in Table 9. Our proposed DR TextSpotter outperforms the state-of-the-art method by about 0.9 % in terms of normalized edit distance, which could verify the effectiveness of our method on the English dataset.



Figure 9: Failed Examples. (a) is caused by the overlapping between different characters. When a part of character crosses with other characters, the model cannot achieve such fine-grained recognition. (b)(c) are caused by the complex layout. In this case, the model is confused with vertical or horizontal order, resulting in misrecognition.

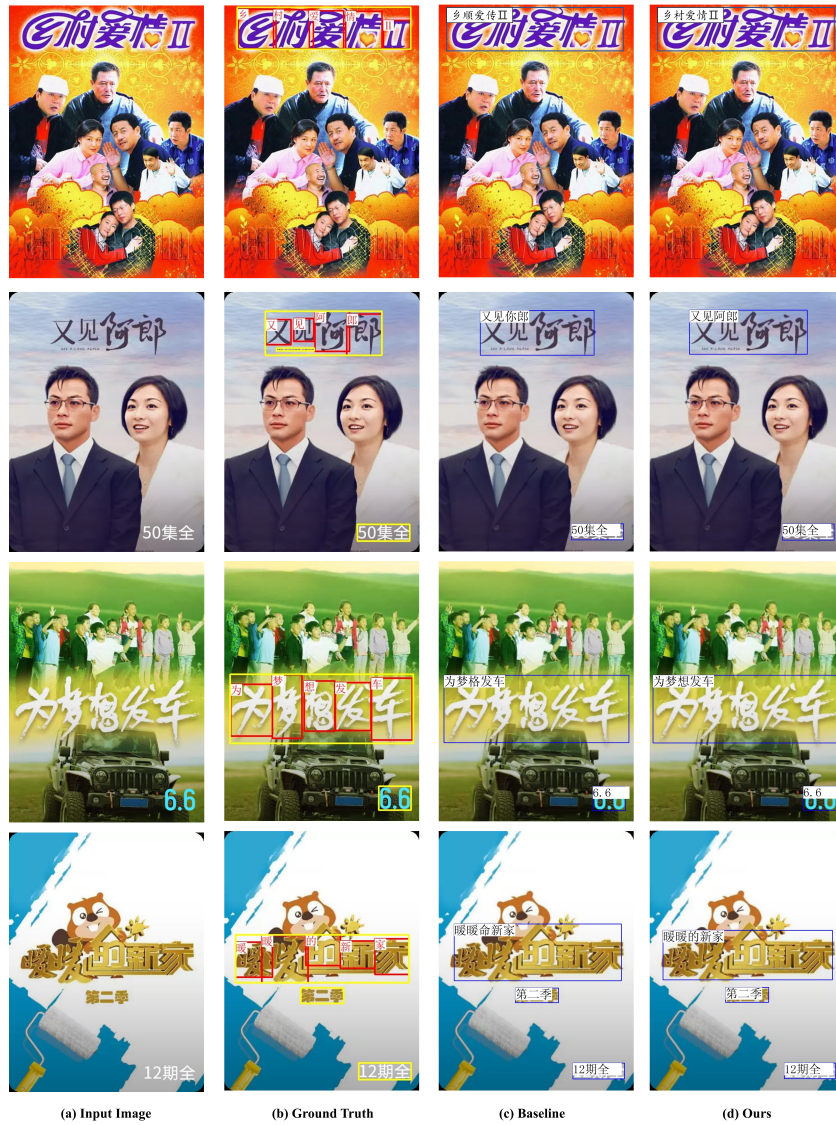


Figure 10: Visualization results on ARText dataset. The baseline is AE TextSpoter w/o LM. More examples can be found in Appendix.

6 Conclusions

The font diversity and shape variance of characters have been ignored in text-spotting tasks for a long time. To remedy this problem, we present a Chinese Artistic Dataset, termed as ARTText, which contains 33,000 artistic images with character-level annotation. Then we propose a deformation robust text spotting method (DR TextSpotter) to detect and recognize text images under the geometric prior. To be concrete, the unsupervised landmark detection sub-network is utilized to highlight the important features as the auxiliary geometric information. Then the graph convolutional network is constructed to fuse this information with the character features, and performs global reasoning to enhance the discrimination of different characters. Experimental results demonstrate the effectiveness of our method on both ARTText and IC19-ReCTS datasets.

References

- [Baek *et al.*, 2019] Y. Baek, B. Lee, D. Han, S. Yun, and H. Lee. Character region awareness for text detection. In *2019 IEEE/CVF Conference on Computer Vision and Pattern Recognition (CVPR)*, 2019.
- [Baek *et al.*, 2020] Youngmin Baek, Seung Shin, Jeonghun Baek, Sungrae Park, Junyeop Lee, Daehyun Nam, and Hwalsuk Lee. Character region attention for text spotting. In *European Conference on Computer Vision*, pages 504–521. Springer, 2020.
- [Cao *et al.*, 2014] Xudong Cao, Yichen Wei, Fang Wen, and Jian Sun. Face alignment by explicit shape regression. *International journal of computer vision*, 107(2):177–190, 2014.
- [Chen *et al.*, 2019] Yunpeng Chen, Marcus Rohrbach, Zhicheng Yan, Yan Shuicheng, Jiashi Feng, and Yannis Kalantidis. Graph-based global reasoning networks. In *Proceedings of the IEEE/CVF Conference on Computer Vision and Pattern Recognition*, pages 433–442, 2019.
- [Cristinacce and Cootes, 2008] David Cristinacce and Tim Cootes. Automatic feature localisation with constrained local models. *Pattern Recognition*, 41(10):3054–3067, 2008.
- [Dai *et al.*, 2017] Angela Dai, Charles Ruizhongtai Qi, and Matthias Nießner. Shape completion using 3d-encoder-predictor cnns and shape synthesis. In *Proceedings of the IEEE conference on computer vision and pattern recognition*, pages 5868–5877, 2017.
- [Do *et al.*, 2022] Tien Do, Ondrej Miksik, Joseph DeGol, Hyun Soo Park, and Sudipta N Sinha. Learning to detect scene landmarks for camera localization. In *Proceedings of the IEEE/CVF Conference on Computer Vision and Pattern Recognition*, pages 11132–11142, 2022.
- [Feng *et al.*, 2019] Wei Feng, Wenhao He, Fei Yin, Xu-Yao Zhang, and Cheng-Lin Liu. Textdragon: An end-to-end framework for arbitrary shaped text spotting. In *Proceedings of the IEEE/CVF International Conference on Computer Vision*, pages 9076–9085, 2019.
- [He *et al.*, 2016] Kaiming He, Xiangyu Zhang, Shaoqing Ren, and Jian Sun. Deep residual learning for image recognition. In *Proceedings of the IEEE conference on computer vision and pattern recognition*, pages 770–778, 2016.
- [He *et al.*, 2017] Kaiming He, Georgia Gkioxari, Piotr Dollár, and Ross Girshick. Mask r-cnn. In *Proceedings of the IEEE international conference on computer vision*, pages 2961–2969, 2017.
- [He *et al.*, 2018] Tong He, Zhi Tian, Weilin Huang, Chunhua Shen, Yu Qiao, and Changming Sun. An end-to-end textspotter with explicit alignment and attention. In *Proceedings of the IEEE conference on computer vision and pattern recognition*, pages 5020–5029, 2018.
- [Huang *et al.*, 2022] Mingxin Huang, Yuliang Liu, Zhenghao Peng, Chongyu Liu, Dahua Lin, Shenggao Zhu, Nicholas Yuan, Kai Ding, and Lianwen Jin. Swintextspotter: Scene text spotting via better synergy between text

- detection and text recognition. In *Proceedings of the IEEE/CVF Conference on Computer Vision and Pattern Recognition*, pages 4593–4603, 2022.
- [Kipf and Welling, 2016] T. N. Kipf and M. Welling. Semi-supervised classification with graph convolutional networks. 2016.
- [Li and Gupta, 2018] Yin Li and Abhinav Gupta. Beyond grids: Learning graph representations for visual recognition. *Advances in Neural Information Processing Systems*, 31, 2018.
- [Li et al., 2017] Hui Li, Peng Wang, and Chunhua Shen. Towards end-to-end text spotting with convolutional recurrent neural networks. In *Proceedings of the IEEE international conference on computer vision*, pages 5238–5246, 2017.
- [Li et al., 2021] Ming Li, Bin Fu, Zhengfu Zhang, and Yu Qiao. Character-aware sampling and rectification for scene text recognition. *IEEE Transactions on Multimedia*, 2021.
- [Li et al., 2022a] Hui Li, Zidong Guo, Seon-Min Rhee, Seungju Han, and Jae-Joon Han. Towards accurate facial landmark detection via cascaded transformers. In *Proceedings of the IEEE/CVF Conference on Computer Vision and Pattern Recognition*, pages 4176–4185, 2022.
- [Li et al., 2022b] Ming Li, Bin Fu, Han Chen, Junjun He, and Yu Qiao. Dual relation network for scene text recognition. *IEEE Transactions on Multimedia*, 2022.
- [Liao et al., 2020] Minghui Liao, Guan Pang, Jing Huang, Tal Hassner, and Xiang Bai. Mask textspotter v3: Segmentation proposal network for robust scene text spotting. In *European Conference on Computer Vision*, pages 706–722. Springer, 2020.
- [Liu et al., 2018] Xuebo Liu, Ding Liang, Shi Yan, Dagui Chen, Yu Qiao, and Junjie Yan. Fots: Fast oriented text spotting with a unified network. In *Proceedings of the IEEE conference on computer vision and pattern recognition*, pages 5676–5685, 2018.
- [Liu et al., 2020] Yuliang Liu, Hao Chen, Chunhua Shen, Tong He, Lianwen Jin, and Liangwei Wang. Abcnet: Real-time scene text spotting with adaptive bezier-curve network. In *proceedings of the IEEE/CVF conference on computer vision and pattern recognition*, pages 9809–9818, 2020.
- [Liu et al., 2021a] Yuliang Liu, Chunhua Shen, Lianwen Jin, Tong He, Peng Chen, Chongyu Liu, and Hao Chen. Abcnet v2: Adaptive bezier-curve network for real-time end-to-end text spotting. *IEEE Transactions on Pattern Analysis and Machine Intelligence*, pages 1–1, 2021.
- [Liu et al., 2021b] Ze Liu, Yutong Lin, Yue Cao, Han Hu, Yixuan Wei, Zheng Zhang, Stephen Lin, and Baining Guo. Swin transformer: Hierarchical vision transformer using shifted windows. In *Proceedings of the IEEE/CVF International Conference on Computer Vision*, pages 10012–10022, 2021.
- [Lyu et al., 2018] Pengyuan Lyu, Minghui Liao, Cong Yao, Wenhao Wu, and Xiang Bai. Mask textspotter: An end-to-end trainable neural network for spotting text with arbitrary shapes. In *Proceedings of the European Conference on Computer Vision (ECCV)*, September 2018.
- [Pedersoli et al., 2014] Marco Pedersoli, Tinne Tuytelaars, and Luc Van Gool. Using a deformation field model for localizing faces and facial points under weak supervision. In *Proceedings of the IEEE Conference on Computer Vision and Pattern Recognition*, pages 3694–3701, 2014.
- [Peng et al., 2022] Dezhi Peng, Lianwen Jin, Weihong Ma, Canyu Xie, Hesuo Zhang, Shenggao Zhu, and Jing Li. Recognition of handwritten chinese text by segmentation: A segment-annotation-free approach. *IEEE Transactions on Multimedia*, 2022.
- [Qin et al., 2019] Siyang Qin, Alessandro Bissacco, Michalis Raptis, Yasuhisa Fujii, and Ying Xiao. Towards unconstrained end-to-end text spotting. In *Proceedings of the IEEE/CVF International Conference on Computer Vision*, pages 4704–4714, 2019.
- [Ren et al., 2015] Shaoqing Ren, Kaiming He, Ross Girshick, and Jian Sun. Faster r-cnn: Towards real-time object detection with region proposal networks. *Advances in neural information processing systems*, 28, 2015.
- [Shi et al., 2018] Baoguang Shi, Mingkun Yang, Xinggong Wang, Pengyuan Lyu, Cong Yao, and Xiang Bai. Aster: An attentional scene text recognizer with flexible rectification. *IEEE transactions on pattern analysis and machine intelligence*, 41(9):2035–2048, 2018.
- [Su et al., 2022] Yuchen Su, Zhiwen Shao, Yong Zhou, Fanrong Meng, Hancheng Zhu, Bing Liu, and Rui Yao. Textdct: Arbitrary-shaped text detection via discrete cosine transform mask. *IEEE Transactions on Multimedia*, 2022.
- [Thewlis et al., 2017] James Thewlis, Hakan Bilen, and Andrea Vedaldi. Unsupervised learning of object landmarks by factorized spatial embeddings. In *Proceedings of the IEEE international conference on computer vision*, pages 5916–5925, 2017.
- [Vaswani et al., 2017] Ashish Vaswani, Noam Shazeer, Niki Parmar, Jakob Uszkoreit, Llion Jones, Aidan N Gomez, Łukasz Kaiser, and Illia Polosukhin. Attention is all you need. *Advances in neural information processing systems*, 30, 2017.
- [Wang et al., 2019] W. Wang, E. Xie, X. Song, Y. Zang, W. Wang, T. Lu, G. Yu, and C. Shen. Efficient and accurate arbitrary-shaped text detection with pixel aggregation network, 2019.
- [Wang et al., 2020a] Wenhao Wang, Xuebo Liu, Xiaozhong Ji, Enze Xie, Ding Liang, ZhiBo Yang, Tong Lu, Chunhua Shen, and Ping Luo. Ae textspotter: learning visual and linguistic representation for ambiguous text spotting. In *European Conference on Computer Vision*, pages 457–473. Springer, 2020.

- [Wang *et al.*, 2020b] Z. Wang, S. Wang, H. Li, Z. Dou, and J. Li. Graph-propagation based correlation learning for weakly supervised fine-grained image classification. pages 12289–12296, 2020.
- [Wang *et al.*, 2021] Wenhai Wang, Enze Xie, Xiang Li, Xuebo Liu, Ding Liang, Zhibo Yang, Tong Lu, and Chunhua Shen. Pan++: Towards efficient and accurate end-to-end spotting of arbitrarily-shaped text. *IEEE Transactions on Pattern Analysis and Machine Intelligence*, 44(9):5349–5367, 2021.
- [Wood *et al.*, 2022] Erroll Wood, Tadas Baltrušaitis, Charlie Hewitt, Matthew Johnson, Jingjing Shen, Nikola Milosavljević, Daniel Wilde, Stephan Garbin, Toby Sharp, Ivan Stojiljković, et al. 3d face reconstruction with dense landmarks. In *European Conference on Computer Vision*, pages 160–177. Springer, 2022.
- [Wu *et al.*, 2017] Yue Wu, Tal Hassner, KangGeon Kim, Gerard Medioni, and Prem Natarajan. Facial landmark detection with tweaked convolutional neural networks. *IEEE transactions on pattern analysis and machine intelligence*, 40(12):3067–3074, 2017.
- [Xia *et al.*, 2022] Jiahao Xia, Weiwei Qu, Wenjian Huang, Jianguo Zhang, Xi Wang, and Min Xu. Sparse local patch transformer for robust face alignment and landmarks in inherent relation learning. In *Proceedings of the IEEE/CVF Conference on Computer Vision and Pattern Recognition*, pages 4052–4061, 2022.
- [Xie *et al.*, 2022] Xudong Xie, Ling Fu, Zhifei Zhang, Zhaowen Wang, and Xiang Bai. Toward understanding wordart: Corner-guided transformer for scene text recognition. In *European Conference on Computer Vision*, pages 303–321. Springer, 2022.
- [Xing *et al.*, 2019] Linjie Xing, Zhi Tian, Weilin Huang, and Matthew R Scott. Convolutional character networks. In *Proceedings of the IEEE/CVF International Conference on Computer Vision*, pages 9126–9136, 2019.
- [Xu *et al.*, 2022a] Chengpei Xu, Wenjing Jia, Tingcheng Cui, Ruomei Wang, Yuan-fang Zhang, and Xiangjian He. Arbitrary-shape scene text detection via visual-relational rectification and contour approximation. *IEEE Transactions on Multimedia*, 2022.
- [Xu *et al.*, 2022b] Chengpei Xu, Wenjing Jia, Ruomei Wang, Xiaonan Luo, and Xiangjian He. Morphtext: Deep morphology regularized accurate arbitrary-shape scene text detection. *IEEE Transactions on Multimedia*, 2022.
- [Yao *et al.*, 2021] Yazhou Yao, Tao Chen, Guo-Sen Xie, Chuanyi Zhang, Fumin Shen, Qi Wu, Zhenmin Tang, and Jian Zhang. Non-salient region object mining for weakly supervised semantic segmentation. In *Proceedings of the IEEE/CVF Conference on Computer Vision and Pattern Recognition*, pages 2623–2632, 2021.
- [Yin *et al.*, 2022] Zihao Yin, Ping Gong, Chunyu Wang, Yizhou Yu, and Yizhou Wang. One-shot medical landmark localization by edge-guided transform and noisy landmark refinement. In *European Conference on Computer Vision*, pages 473–489. Springer, 2022.
- [Zhang *et al.*, 2019] Rui Zhang, Yongsheng Zhou, Qianyi Jiang, Qi Song, Nan Li, Kai Zhou, Lei Wang, Dong Wang, Minghui Liao, Mingkun Yang, et al. Icdar 2019 robust reading challenge on reading chinese text on signboard. In *2019 international conference on document analysis and recognition (ICDAR)*, pages 1577–1581. IEEE, 2019.
- [Zhao *et al.*, 2021] Yifan Zhao, Ke Yan, Feiyue Huang, and Jia Li. Graph-based high-order relation discovery for fine-grained recognition. In *Proceedings of the IEEE/CVF Conference on Computer Vision and Pattern Recognition*, pages 15079–15088, 2021.